POLITECNICO DI MILANO
Master of Science in Telecommunication Engineering
Electronic, Information and Bioengineering Department

Air to Ground Channel Characterization in an Indoor-to-Outdoor Scenario

Supervisor: Ing. Maurizio Magarini
Advisor: Ing. Roberto Nebuloni

Master of Science Degree Thesis by:
Lorenzo Norberti
Student ID: 900073

Academic Year 2018-2019

"Proprio come un fiore sboccia dopo aver sopportato
il rigido freddo invernale, un sogno può avverarsi solo
se si è preparati a sopportare i tormenti che ne accompagnano la
realizzazione e a compiere tutti gli sforzi necessari.
Perciò sii paziente verso quanto ti accade,
curati e amati senza paragonarti o voler essere un altro fiore,
perché quando ciò accadrà,
potrai scoprire che andavi sognando
di essere un fiore che aveva da fiorire."
Daisaku Ikeda

Acknowledgment

Alla fine di questo percorso che, ponendomi davanti ostacoli e mettendo alla prova spesso e volentieri la mia determinazione, ha sicuramente avuto un ruolo nel formare la persona che sono oggi, desidero fare alcuni ringraziamenti. Il primo va sicuramente i miei genitori e la mia famiglia, dai quali non è mai mancato il sostegno soprattutto nei momenti in cui era più semplice abbattersi e rinunciare, che mi hanno insegnato a credere sempre nelle mie potenzialità e permesso di intraprendere questo percorso senza negarmi mai il loro appoggio.
Ringrazio il Prof. Magarini per la possibilità concessami nello sviluppare un lavoro così stimolante e per il supporto fornitomi.
Grazie ad Andrea e Guido, i fratelli non di sangue che ti scegli, con i quali ho condiviso gioie e dolori, la vita e i diversi percorsi intrapresi ci hanno spesso allontanato ma mai diviso e anzi, sempre ancor di più unito.
Grazie agli amici di una vita, dai quali talvolta ho ricevuto l'amicizia nella forma più frivola ma sempre la più vera, che non mi hanno mai giudicato nelle sconfitte ma dai quali ho sempre saputo di poter avere una mano nel momento di necessità senza che ci fosse mai bisogno di chiedere niente, "Ci si infamerà ma ci si vuol bene".
Grazie invece a coloro che ho scoperto per ultimi ma che non per questo sono meno importanti, grazie al gruppo "una bevutina easy", garanzia di danni e buon umore ma sempre disponibili per una parola di conforto.
Grazie a Celeste, sempre capace di farmi ritrovare tranquillità, il sorriso e mai banale in ogni sua parola o consiglio. Grazie a tutti voi.

Abstract

In this thesis I focused on an Air-to-Ground transmission, where the communication takes place in an urban environment from a terminal inside a building towards outdoor unmanned aerial vehicle (UAV) or drone, with mini base station on board. The motivations behind this study are referred to the progressive increasing damages trend caused by natural disasters and emergency situations that cause damage to the traditional network infrastructure, inducing the consecutive necessity to explore alternative communication systems.

In this sense, in order to establish a real time interactivity with UAVs, the 5G evolution can be the key that allows us to explore new solutions providing higher data speed and low-latency improvements compared to 4G and 4.5G (LTE advanced) technologies.

The channel characterization has been the main contribution of this analysis, this allows to study both the link quality, which is a performance indicator for a proper reception of the signal and it is necessary to ensure the aerial wireless services to the affected users, and the necessity to provide the maximum signal coverage.

The characterization was conducted by using Wireless Insite ray-tracing software, through which I carried out an inspection on the distribution of the received power density w.r.t receivers positions. Also, I studied the direction of arrival in terms of angle of arrivals, obtaining results that can be used in future to improve performance.

Angle of Arrivals are positional information that can be extracted via mea-

surements observed and contextual data and can be useful to formulate and develop new localization approaches that may allow to quickly locate people.

Contents

List of Figures

Chapter 1

Introduction

"Climate change has been strictly connected with an increase in the frequency and intensity of natural disasters in many regions" was the assumption that researchers demonstrated in 2019 in their article [1] published on The Proceedings of the National Academy of Sciences (PNAS).
In this work they document an increasing trend in extreme damages from natural disasters in parallel with the rise of costs and resources used to cope with assistance and rescue of the people involved.

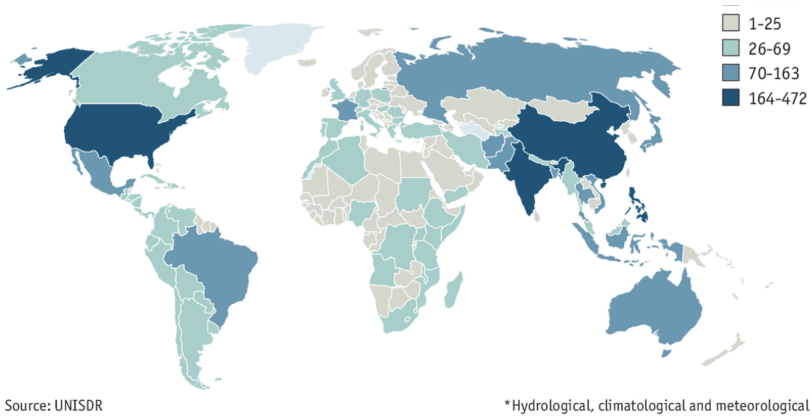

Figure 1.1: Total numbers of natural disasters reported per country, 1995-2015.*

Luckily another conclusion, based on the data considered in their analysis, is that the mortality percentage is on a downward trend also thanks to the improvement of early warning systems, evacuation schemes and more effective relief efforts.
Since these aspects have became more and more critical many scientist focused their attention in order to explore alternative systems, employing the most modern technologies to cope with the necessity of contacting survivors trapped in the buildings when communication infrastructure could be severely damaged, become dysfunctional due to failure of different sub-system interconnections, or physical network components could be broken.

1.1 Urban Disaster and Emergency Communication Systems

In [2] previous works have been developed as in the case of [3], where the concept of spatial and time changes rate in the measurement of wave propagation has been investigated and a propagation model considering distance and frequency in micro-cell downtown environment was proposed.
The main idea in [2] was to consider natural disaster event such as cyclone, flood, or earthquake where it could happen that missing people are trapped inside single or multi-floor buildings (offices and houses) and need to be located or to contact the rescue units.
In recent years we have seen the design and development of increasingly reliable Drones and Aerial Vehicles (UAV) that are destined to evolve into daily custom accomplices also thanks to the increasingly affordable prices. In fact they have become widely enforced in many activities, both military and civilian, which include from land control to criminal monitoring, from analysis of the land to the search for missing people after a natural disaster.
In this context, also the evolution of the new 5G communication technology allows us to go beyond the limits of a Wi-Fi or LTE connection such as the

low reliable and high-latency transmission, giving us the possibility to control remotely cluster of Drones and Remotely Piloted Aerial System (RPAS). One of the most important targets of the 5G technology is to guarantee an Ultra Reliable and Low Latency Communication (URLLC) that is indispensable for high profile real-time employment of every kind of remote controlled (RC) apparatus.

Right in such scenarios these quasi-stationary aerial platforms could emerge also as a viable and cost-effective solution to provide temporary cellular and broadband services in order to establish an end-to-end connection between the rescue team and back-end control station.
This implementation, where a UeNB (micro base station) can be manage to fly on a drone above the affected area, presents significant advantages over the conventional methods in line with the broadband cellular concept:

- Rapid deployment covering a large geographical area
- High flexibility of the position of the receivers due to the high capability of movement of drones in the air
- Immunity to disasters
- Possibility to establish a good link quality between nodes due to the of the opportunity to ensure also a Line Of Sight (LoS) link between nodes thanks to the drone movement.

- Better signal propagation than terrestrial solutions due to higher altitude

1.2 Research Methodology

We realize the settlement of our scenario thanks to Wireless InSite, a multifunction radio wave propagation simulator that integrates a suite of ray-tracing models and high-fidelity EM calculators for the analysis of site-specific radio wave propagation and wireless communication.
Thanks to the wide range of tools available in the software it permits the prediction of the effects of buildings and terrain during the electromagnetic waves transmission through the implementation of the ray-tracing techniques.
The application of the ray tracing technique in communication systems field analysis occurred since in a wireless transmission signal propagates through multiple paths caused by ground and building walls reflections, diffractions, or penetrations, each one with specific peculiarities like different times of arrival, phase condition or paths length [7]. In particular, it allows to understand how the locations of the transmitters and receivers within an urban area affect signal strength.
It gives the capability to model the physical characteristics of irregular terrain and urban building features, it performs the electromagnetic calculations, and then it evaluates the signal propagation characteristics.
At each receiver location, many contributions generated from different ray paths are combined and evaluated to determine desired outputs.
In the initial stage, to ensure the reliability of results obtained, we have conducted a phase in which we have applied, in parallel with the software outcome, an analytical analysis of the results through the study of propagation models already developed that could better describe or approximate our environment.

In the end, after acquiring a sufficient set of data that would allow us to get verifiable results, we proceed to data analysis using Matlab to process the informations.

1.3 Thesis Objectives

Most of the previous papers and articles, which will be cited in the bibliography section and are taken as a reference during the development of this thesis, have focused their study on an urban outdoor simulation environment in which, in order to simplify the calculation and simulation, they do not consider the penetration of the signal through the walls of the buildings, the consequent power magnitude reduction of the wave but also the addition of multiple paths deriving from this phenomenon. In fact, in order to obtain an applicable model for various simulation environments that would simplify the estimate of radio coverage, they focus their attention exclusively on the impact of reflection and diffraction phenomena.

My study aims to evaluate the air to ground channel characterization for an indoor-to-outdoor scenario, with special focus on the attenuation criticality derived from the interaction of the signal with the internal structure of the building.
My results will be mainly divided in three parts:

- In the first one I am going to apply the principles of regression and curve fitting on the data collected array in order to obtain a linear model and, consequently, an approximated curve which gives us an indication on the trend of the received power with respect to the distance.
- In the second part I will still consider the received power extrapolating, thanks to the use of Matlab, an estimation of the power received distributions w.r.t receivers sensitivity.

- The last result will concern the evaluation of the direction arrivals, parameter that can give us an indication as regards the location of the transmitters (and therefore of the missing people) inside the building. Indeed conventional localization approaches typically rely on the estimation of single values, such as distances and angles from inter-node measurements which can be hard to be obtained, especially in harsh wireless propagation environments.

All these analysis have been done checking, through data comparison, how the different positioning of the receivers along the sides of the building impacts the values of the measurements and and therefore the results obtained.
In the first chapter we are going to synthesize a short review on the basic theory behind the analysis we treated in this thesis. Indeed the physics of Electromagnetic Fields together with Optics fundamentals gives us the possibility to better understand the principles behind the phenomena of transmission, reflection and refraction caused by the propagation of an electromagnetic wave from one medium to another. We end this part considering two direct applications of what we have cited so far.
In the second chapter we introduce and discuss first the main reasons behind our analysis, in fact it has been conducted due to the progressive increasing damages trend caused by natural disasters with the consecutive necessity to explore alternative communication systems. The description of the techniques adopted follows, then we proceed with a brief overview about other works connected with the pattern we have faced, illustrating the channel models used to advance the link investigation and after all we address the characterization of scenario we have created focusing the attention in particular on the study of the transmission channel and its peculiarities.
In the fourth chapter the analysis of the scenario we implemented through the use of Wireless InSite is described, starting with a brief introduction on the program, models adopted and their peculiarities and then the description of the outputs request and the derivation explaination through analytical formulas.

Last chapter is characterized by the exposure and summary of the results obtained with a quick presentation about the organization of themselves.

Chapter 2

Electromagnetic waves Propagation

In this chapter we are going to synthesize a short review on the basic theory behind propagation of electromagnetic waves. In fact, the physics of Electromagnetic Fields together with Optics gives us the possibility to better understand the principles related to the phenomena of transmission, reflection and refraction caused by the propagation of an electromagnetic wave from one medium to another. The chapter ends considering two direct applications of what we have cited so far, which are:

- Propagation through a dielectric layer
- Transmission through a wall

the applicability of which allows us to design and understand more complex analysis situations like, for example, an indoor to outdoor propagation in an urban environment.

2.1 References on Maxwell Equations

In 1873 Maxwell published his seminal work, the "Treatise on Electricity and Magnetism" in which appeared for the first time the equations regulating the electrical and magnetic field behavior [4].

$$\nabla(E) = 0 \tag{2.1}$$

$$\nabla(B) = 0 \tag{2.2}$$

$$\nabla \times E = -\frac{\partial B}{\partial t} \tag{2.3}$$

$$\nabla \times B = \varepsilon\mu\frac{\partial E}{\partial t} \tag{2.4}$$

E and B are electric field and magnetic field vectors and ε and μ are dielectric function and absolute permeability of the physical medium. If we fix the attention on the electric field we can obtain that the solution of the wave equation (obtained from Maxwell equations) is a periodic travelling wave that can be expressed in a exponential form with complex exponent.

$$E = E_0^{i(k\cdot r-\omega\cdot t+\varphi)} \tag{2.5}$$

where k is the wave vector $k = 2\pi/\lambda$ oriented towards the wave propagation direction, ω is the pulsation equal to $2\pi f$, f is the frequency and φ is the initial phase. Electric and magnetic fields vibrate in a plane perpendicular to the direction of propagation, being always perpendicular to each other, and the ratio between them is equal to the velocity of the wave given by $v = \lambda/T = \omega/k$ with T period in second.
On the other side the one between E and the magnetizing field H is:

$$E/B = v \tag{2.6}$$

$$E/H = E\mu/B = \sqrt{\mu/\varepsilon} = Z \tag{2.7}$$

Z is called characteristic impedance of the material and for the vacuum (Z_0) is equal to 377 Ω

2.1.1 Electromagnetic wave from one medium to another

The continuity conditions at each point of the separation surface that must be respected from a wave traveling from one medium to another are:

$$E_{1t} - E_{2t} = 0 \qquad D_{1n} - D_{2n} = \sigma \tag{2.8}$$

where E_{1t} and E_{2t} are the Electric field vector components tangent to the surface in the 1st and 2nd medium and D_{1n} and D_{2n} are the those of the vector normal displacement to the surface,σ is the surface density of electric charge. For the magnetic field instead:

$$H_{1t} - H_{2t} = J_s \qquad B_{1n} - B_{2n} = 0 \tag{2.9}$$

where J_s is the density of surface current. If there are no charges, conservation is found on the border between the two mediums of the components tangent E and H and normal D and B.

2.2 The Fresnel equations

Let us consider the case of an electromagnetic plane wave with pulsation ω_i that hits the surface between two dielectric mediums with an angle θ_i.
We suppose the common case in which the magnetic permeability can be considered approximately equal to the vacuum case, for this reason from the definition of the refractive index n, as ratio c/v between speed of the light in vacuum and in the medium, we can express $n_i = \sqrt{\varepsilon_i}$, where ε_i are the dielectric relative constants of the mediums.

2.2.1 Plane wave incidence on dielectric interface

Experimentally we know that part of the wave is reflected and part is refracted and penetrates into the second medium. The continuity of the fields can be expressed also by $E_i + E_r = E_t$ and $H_i - H_r = H_t$, so at the border between the two mediums the electric field splits into two terms, one for the reflected wave

$$E_r = E_{0r}^{i(k_r r - t\omega)} \tag{2.10}$$

and another transmitted/refracted wave

$$E_t = E_{0t}^{i(k_t r - t\omega)} \tag{2.11}$$

In order to respect the condition of equality and continuity of the fields at the boundary, it was considered both the same ω pulsation for E_i, E_r and E_t which correspond, for any instant t, to the equality of the exponential arguments ($k_i \cdot r = k_r \cdot r = k_t \cdot r$).
The wavelenght is given by $\lambda = 2v\pi/\omega$, so we obtain that

$$\lambda_i = \lambda_r \qquad \lambda_t = \frac{n_1}{n_2}\lambda_i \tag{2.12}$$

At this point we can state that the three wave vectors k_i, k_r and k_t lie on the same plane and, by expressing in terms of wavelengths and keeping in mind $\lambda_r = \lambda_i$ we have:

$$\frac{2\pi}{\lambda_i}\sin\theta_i = \frac{2\pi}{\lambda_i}\sin\theta_r = \frac{2\pi}{\lambda_t}\sin\theta_t \tag{2.13}$$

So at the end, considering $\lambda_t/n_1 = \lambda_i/n_2$

$$\theta_i = \theta_r \quad \textit{and} \quad n_1\sin\theta_i = n_2\sin\theta_t \tag{2.14}$$

This is called *Snell-Descartes Law* or *Law of Refraction* and in addition to describing the relationship between the angles of incidence and refraction between two different isotropic media, it indicates that the refracted radius is closer to normal if the second medium is more reflective than the first and vice versa.

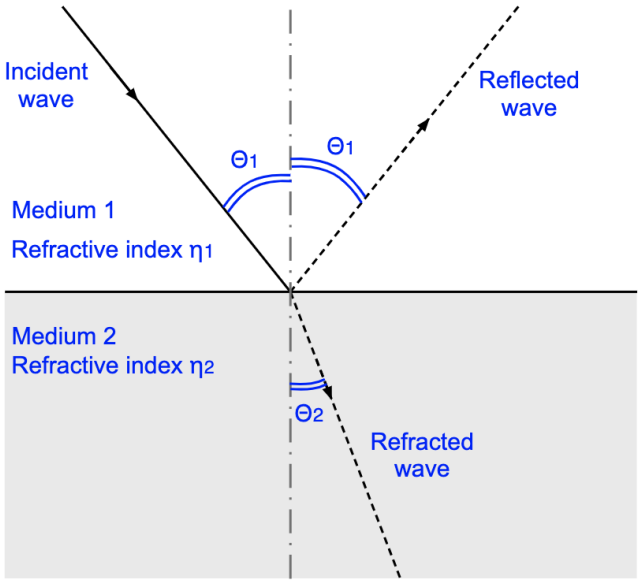

Figure 2.1: Propagation of reflected and refracted waves.

2.2.2 Reflection and Transmission coefficients

The continuity relations (2.8) and (2.9) that we have seen [4] can also bee written in terms of corresponding electric fields using 2.7, the characteristic impedances of the two media:

$$\frac{E_i - E_r}{Z_1} = \frac{E_t}{Z_2} \qquad so \qquad E_i - E_r = \eta E_t \tag{2.15}$$

thanks to the introduction of the parameter $\eta = Z_1/Z_2 = n_2/n_1$.
These equations constitute a linear system that can be easily solved according to the E_i field, providing the relationships

$$E_r = \frac{1-\eta}{1+\eta} E_i \quad and \quad E_t = \frac{2}{1+\eta} E_i \tag{2.16}$$

that gives the amplitude of the electric field of the reflected and transmitted wave depending on the incident wave. From these we can define the coefficients of reflection and transmission, such as

$$r = \frac{E_r}{E_i} = \frac{1-\eta}{1+\eta} \qquad t = \frac{E_t}{E_i} = \frac{2}{1+\eta} \tag{2.17}$$

Let's discuss some consequences: While t is a real quantity always positive, reflection coefficient r is also real, but can be positive or negative depending on whether η is less than or greater than 1. This means that transmitted field is always in phase with the incident field, while reflected field is in phase if $n_1 > n_2$ and is in counterphase if $n_1 < n_2$.
We need to pay attention not to confuse these coefficients, expressing the relationships between the fields, and the same amounts that express instead the relationship between the intensity:

$$I = \frac{E^2}{2Z} \qquad R = \frac{I_r}{I_i} = r^2 = (\frac{1-\eta}{1+\eta})^2 \qquad T = \frac{I_t}{I_i} = \frac{Z_1}{Z_2} t^2 = \frac{4\eta}{(1+\eta)^2} \tag{2.18}$$

2.2.3 Application: dielectric layer

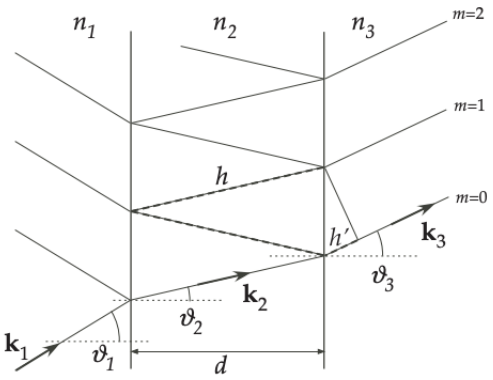

Figure 2.2: Multiple reflections of a plane wave on dielectric layer.

Let's see the situation in which the refractive index of the first and third medium (n_1 and n_3) are supposed to be equal and different from n_2 [5]. Because of what we've seen about transmission on a dielectric interface[4], thanks to 2.14 we can state that the pulsation of the radiation must be the same in all the media, so the following relations are valid:

$$\frac{k_1}{n_1} = \frac{k_2}{n_2} = \frac{k_3}{n_3} = k_0 \qquad n_1 \sin\theta_1 = n_2 \sin\theta_2 = n_3 \sin\theta_3 \tag{2.19}$$

where $k_0 = 2\pi/\lambda_0$, and λ_0 is the wavelenght in vacuum.
The amplitudes of the waves reflected and transmitted by the layer can be calculated by assessing the interference between the infinite flat waves produced by the multiple reflections on the separation surfaces between means. Let's call with r_{ij} and tij the reflection and transmission coefficient for a wave coming from the medium i and incident on the medium j. As we know

$$r_{ij} = \frac{1-\xi_{ij}}{1+\xi_{ij}} = -r_{ji} \qquad t_{ij} = \frac{2}{1+\chi_{ij}} = \chi_{ji} t_{ji} \tag{2.20}$$

$$\text{with} \qquad \chi_{ij} = \tfrac{n_j \cos\theta_j}{n_i \cos\theta_i}$$

The first wave (m=0) is simply transmitted from the two surfaces and therefore, at the exit it will have an electric field:

$E_t^0 = E_i t_{12} t_{23} e^{i\varphi}$ where E_i is the incident field propagating towards θ_3.

φ is the phase shift due to the propagation inside the layer by considering a plane wave that spreads for a length d (slab thickness) with wave vector $k_2 = n_2 k_0$ and directed by the orientation identified by θ_2 w.r.t z axis.
It is $\varphi = d n_2 k_0 \cos\theta_2$

The second wave (m=1) will take a different path with respect to the first one so, in addition of the contribute of the reflection from the two surfaces of the layer given by a multiplication of the amplitude by the factor $r_{23} r_{21}$, it will have a 2φ phase shift:

$E_t^1 = E_i t_{12} t_{23} (r_{23} r_{21}) e^{i3\varphi}$

Iterating the process, the amplitude of the transmitted wave will result:

$$E_t = E_i t_{12} t_{23} e^{i\varphi} \sum_{m=0}^{\infty} ((r_{23} r_{21}) e^{i2\varphi})^m = E_i \frac{t_{12} t_{23}}{1 - r_{23} r_{21} e^{i2\varphi}} = E_i \cdot t \qquad (2.21)$$

2.2.4 Application: Free space propagation with wall obstacle

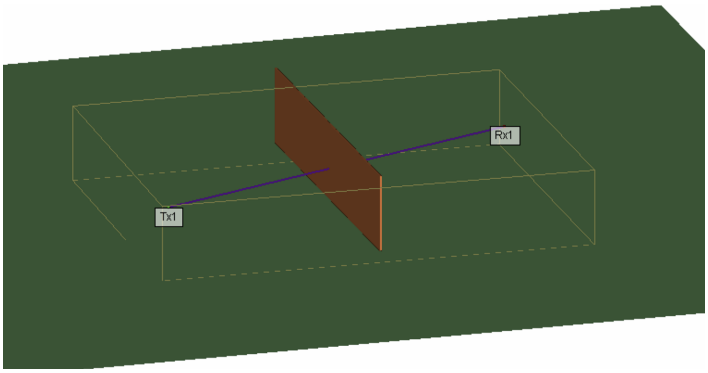

Figure 2.3: Transmission through a wall.

The introduction of the previous application [5] with the consecutive result of the analysis (2.21) gives us the possibility to investigate the case in which a physical obstacle (or simply a wall) interposed between transmitter and receiver is crossed during transmission in free space.
Free space propagation model is the simplest scenario for the propagation of radio signals, it is the result of a LoS (Line of sight) path with no obstacles nearby to cause reflection or diffraction where is assumed that the electric field decreases as $1/r$ with distance in all directions. The standard form of the Received Power Pr from the Rx antenna with Gain G_r at a distance d from a Tx with gain G_t and Output Power P_t is:

$$Pr(d) = \frac{P_t G_t G_r \lambda^2}{(4\pi d)^2} \tag{2.22}$$

The problem is easier to be solved if we consider, as a first approximation given the distances involved, the coupling between the antennas in free space. In this case the attenuation due to the insertion of the slab can simply be subtracted in dB ($t_{dB} = 20log[t]$).

$$Pr_{tot} = Pr_{dB}(d) + t_{dB} \tag{2.23}$$

Chapter 3

Architecture Design

In this chapter I introduce and discuss first the reasons behind the need to examine the critical issues arising from the air-to-ground transmission analysis within an urban context and the techniques adopted.
Then, I proceed with a brief overview about other works connected with the pattern that I've faced, describing channel models used to advance the link investigation and, later on, I address the description of scenario that have been created focusing in particular the attention on the study of the transmission channel and its characteristic.

3.1 Channel Modelling

Channel model is a mathematical representation of the impact that the communication channel have on the wireless signals propagation. It is essential for evaluating the performances of wireless communication systems because it reflects the signals propagation components in radio environments.
The application of the right channel model allows to provide a realistic assessment of the system and can constitute a significant support to optimize the link performance.

Three channel elements compose and heavily affect the performance of the overall channel model of a wireless system :

- *Path loss*: main large scale item, characterized by a deterministic relation between distance and the mean attenuation in a given environment. It decreases almost linearly in dB with log(d).

$$PL = C\Big(\frac{d}{d_0}\Big)^{\mu} \tag{3.1}$$

  where C is the attenuation at the reference distance d_0 and m is the path loss coefficient.

- *Shadowing*: random fluctuations of the attenuation around the path loss (called also large scale fading). They are given by the presence of large obstructions like buildings which shadow completely or partially the propagation path. It is well described by a log-normal distribution.

$$f_{SH}(A_{SH}) = \frac{1}{\sqrt{2\pi\sigma_{SH}^2}} e^{(\frac{-(A_{SH}-\mu)^2}{2\sigma_{SH}^2})} \tag{3.2}$$

  where μ is the mean, A_{SH} is the additional attenuation in dB and σ_{SH} is the standard deviation in the dB domain (between 2 and 8 in typical urban environments).

- *Multipath fading*: signal propagates from the source to the destination through multiple different paths due to obstacles and reflections existing in the wireless channel. All these waves are combined at the receiver and a random attenuation fluctuations around the large scale attenuation (path loss + shadowing) is introduced.
  In presence of dense multipath the contributions summation can be treated as a normal (Gaussian) distribution, hence we identify two propagation conditions that are the fundamental of the most part of the wireless multipath channel models:

- absence of dominant path (non-line-of-sight condition)

- presence of a dominant path (line-of-sight condition).

After making this distinction, the two cases are analyzed differently, using *Rayleigh distribution* for LoS case and then applying *Ricean distribution* for NLoS condition.
In [5] they investigate different pathloss models for UAV based wireless communication networks, choosing the best one for the case studied and adapting it to capture the effects of indoor obstacles and blockages.

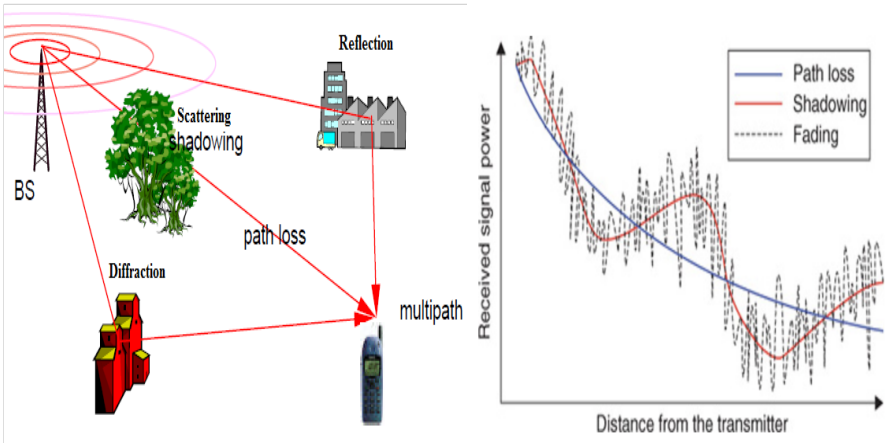

Figure 3.1: Representation of the large-scale (path loss and shadowing) and small-scale (fading) propagation effects.

3.2 Link Analysis

A fundamental aspect to take into account, which gives an indication of how good a communication channel is for transmission and proper reception of signals, is the characterization of the link quality. Indeed it must be provided with highest possible accuracy to guarantee the aerial wireless services to the affected users, developing models that can capture both the uplink

and downlink channels. The reason is that performances of communication protocols in terms of efficiency and Quality of Service are directly connected to the channel characteristics.

The end-to-end transmission between mobile terminals and Drones thus can be divided into two parts:

- Indoor part
- Outdoor part

This is done to differentiate indoor propagation distance from trapped users' position till the exposed wall and the outdoor distance from the exposed wall to the Drones.

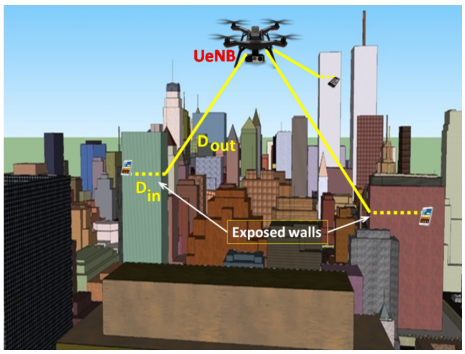

Figure 3.2: Urban Airborne Communication Scenario.

Indoor part of the wave propagation gets consistently influenced by the internal structure as the dimensions and position of walls, the density of fornitures and construction materials, while the outdoor part, depending on the frequency used, can be more or less affected by atmospheric components such as temperature or humidity and by the exposing to weather conditions which may cause severe degradation in system performance due to scattering phenomenon.

In an aftermath disaster aerial communication network pathloss characteristics are a combination of indoor and outdoor paths and due to different propagation environments and time varying nature of the signal propagation, uplink and downlink signal transmissions are not symmetrical:

Uplink Channel

1. Two-ray model - Uplink [6]:

$$PL_{UL,T}(dB) = -10\log_{10}\left[\left(\frac{\lambda}{4d\pi}\right)^2[2\sin\left(\frac{2\pi h_t h_r}{\lambda d}\right)]^2\right] \tag{3.3}$$

2. Winner II - Uplink [7]:

$$\begin{aligned} PL_{UL,T}(dB) = (44.9 - 6.55\log_{10}(h_{BS}))\log_{10}(d_{in} + d_{out}) + \\ +34.46 + 5.83\log_{10}(h_{BS}) + 23\log_{10}(f_c/5.0) + 17.4 + 0.5(d_{in}) - \\ +0.8(h_{MS}) + L_o \end{aligned} \tag{3.4}$$

Downlink Channel

1. FSPL - Downlink [8]:

$$PL_{DL,F}(dB) = 32.45 + 20\log_{10}(d) + 20\log_{10}(f) \tag{3.5}$$

2. Winner II - Downlink [7]:

$$\begin{aligned} PL_{DL,W}(dB) = 40\log_{10}(d_{in} + d_{out}) + 13.47 - \\ +14\log_{10}(h_{BS} + h_{MS}) + 6\log_{10}(f_c/5.0) + 17.4 + 0.5(d_{in}) - \\ +0.8(h_{MS}) + L_o \end{aligned} \tag{3.6}$$

where
h_{BS}= height of UAV
d_{out}= aerial distance of users to drones
d_{in}= indoor distance of the users in building
h_{MS}= height of mobile station
f_c= frequency in GHz
L_o= additional indoor pathloss factor due to the indoor obstacles

3.3 Ray Tracing

The basic idea behind ray tracing was already born in the 16th century and has existed for decades, but only in the last few years there has been an increase in interest thanks to the growth in the number of fields in which it can be used such as, for example, the realization of visual effects in films and television but also in real-time applications like video games.
As well explained in many articles [9], it is a three-dimensional computer graphics rendering technique, which is able to produce images with a high degree of visual realism taking advantage by very complex light interactions, in fact, it is based on the main idea that, leveraging reflection and refraction concepts we introduced previously (2.2.1 and 2.2.2), we can model them and a variety of other optical effects by following the path that light rays takes as it bounces through an environment.
The benefits of implementing this technique are numerous, in fact it is able to add more realism to ray traced images introducing authentic simulations on the geometry of interest and, thanks to that, effects which are hard to be simulated using other algorithms are a direct result of the ray tracing algorithm. On the other hand the drawback is given by the greater computational cost w.r.t typical scanline rendering methods or other algorithms, this was the reason why until few years ago it was considered a technology not suitable for real time applications (as videogames) that needed low la-

tency.

Previous usefull statistical models used so far didn't provide site-specific information during the propagation characteristics estimation while the use of this technique it is possible through the request of three important specification: the propagation distance, the incident angle on the surfaces, and permittivity of the reflecting materials (first two are obtained from estimation results).

I used in my study Wireless Insite, an electromagnetic simulator that supports the RF engineers with the tools necessary to design wireless links, to optimize antenna coverage and to assess key channel and signal characteristics. During the setting phase it gives us the possibility to chose between two ray tracing methods: *Shooting and Bouncing Ray method* (SBR) and *Eigenray method*.

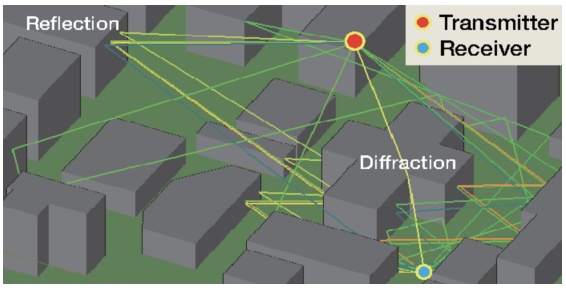

Figure 3.3: Example of ray-tracing application in electromagnetic propagation.

Shooting and Bouncing Ray (SBR):

The SBR method is used to trace ray paths through the building geometry without considering the position of specific field points. Rays are traced from the transmitter reflecting identically on the building walls and continue to be traced up to the maximum number of reflections until they reach the receiver. Once the paths are created, the destinations of each segment are saved in a file in the study area folder together with the sequence of interactions and then used to calculate the electric field strength.

computation time is proportional to: $\frac{(N_R+N_T+1)!}{N_R!N_T!}$

where N_R is the number of reflections and N_T the number of transmissions. When diffractions are considered, computation time is approximately proportional to the number of facets squared.

Eigenray method:

This procedure involves a direct disposition of the ray paths between each source and destination that satisfy Fermat's Principle of least time. The Eigenray method is limited to ray paths with up to three reflections and diffractions and like SBR scheme, it take into account up to 30 transmissions per ray path.

computation time is comparable to: $(N_F)^{\chi}$

where N_F is the number of facets, and χ is the maximum number of reflection and diffraction interactions on any path, with the peak equal to three.

3.4 Related Works

As presented in [10], an essential element for efficient dimensioning of a system of communication is the planning tool, which however provides only outdoor coverage predictions, indeed it generally estimates the path loss from the Base Station (BS) to the position where external terminals are assumed to be with particular attention to link budget design.
Therefore, the evaluation of an extra signal attenuation parameter associated with building penetration is required during the planning of the network and it is often poorly considered, so an accurate analysis of the indoor propagation can lead to determine distinct attenuation value for this loss parameter that can improve the indoor to outdoor coverage for a certain percentage of

indoor ambiences.
This estimation can be obtained via propagation models or through predictions extracted from measurement campaigns.
A fairly large number of articles from the past, as [8] for example, took into account during the study, as we have seen especially in sections 3.1 and 3.2, outdoor urban environments.
Just in [8] many improvements have been reached developing previous works, in fact researchers started from [11] where authors simply consider LoS condition between aerial base station and receivers, proceeding with [12] where the introduction of three additional classes of links (LoS, OLoS and NLoS) have been proposed and consequently pathloss models based on them have been designed.
Especially in this paper they setted up an outdoor urban environment where large-scale buildings were considered as solid blocks discarding the propagation by penetration throught walls that would have a significant impact on the model. In order to cover a different range of application, they separate 4 scenery (Suburban, Urban, Dense Urban and Highrise Urban) setting differently the parameters associated to each ambiance (ratio of buildt up, mean number of buildings and buildings heights distribution).

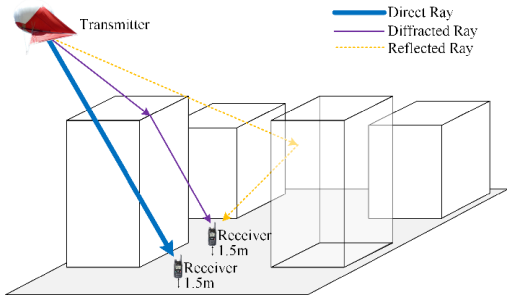

Figure 3.4: Urban layout and types of simulated rays.

They estimated the infrastructure required to establish the desired service and they have executed the modelling of the urban environment layout and characteristic of the building, neglecting the disposition of additional possible elements like trees or mobile objects to simplify the calculation.
In the end they presented a statistical Air-to-Ground RF propagation model for low-altitude platforms in an outdoor urban environments that can facilitate the planning efforts of airborne wireless services.

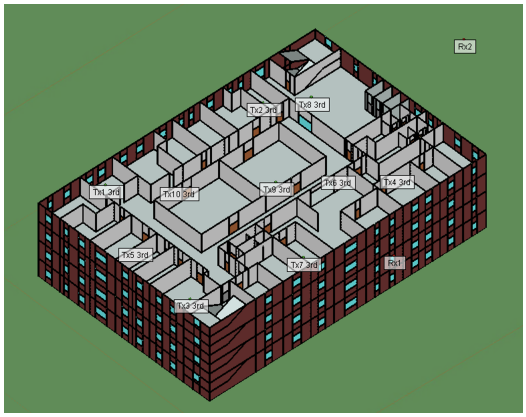

Figure 3.5: Realization of building with complex floor.

3.5 Single Building Scenario

Urban Indoor-to-Outdoor environment requires, in particular during the analytical analysis setting phase, the addition of supplementary parameters and principally ad hoc models development to reproduce and approximate the complexity of the situation. In fact the already known RF models can be usefull for the designers to speed up radio coverage estimation and calculate the expected pathloss (used to produce numerous data such as SINR and expected throughput) but they cannot match the accuracy of site-specific ray tracing simulations.

In our scenario I implement, with the support of the ray-tracing simulation software, a condition which is rarely taken into consideration and so therefore needs a meticulous initial setting phase to ensures the results obtained. Indeed an NLoS transmission between an indoor users and an Air-Drone flying outside presents many criticalities, as the necessity to formulate standard models to express non-symmetrical links, the presence of obstacles and losses given by the architecture and the signal interactions with obstacles that are totally absent in other situations.

Floor Plan Editor Tool allows the user to create a customized indoor environ-

ment by specifying wall locations, heights and peculiarity of ceilings, floors, windows and doorways. Material properties of each of these structures can be changed to accurately reflect the real environment in the most likely way possible.
In my ambiance I realized a 4-floor parallelepipedal building through the duplication of a complex plan initially implemented, setting each floor to 4 m high, the longest side of 60 m and the shortest side of 40m. Thickness and materials chosen for the walls, windows, doors, ground and ceiling of each floor plan are set separately, including the electromagnetic properties that vary from each other depending on the selected substance (as we can see in table 3.1) and for this reason affects differently the wave propagation subject to frequency.

Material	**Permittivity**	**Conductivity**	**Thickness**
Brick	4.44	0.001	0.25
Concrete	15	0.015	0.3
Wood	5	0	0.03
Glass	2.4	0	0.003
*Layered Drywall	2.8 and 1	0.001 and 0	0.125

Table 3.1: Characteristics of used materials.

* construction material consisting of thin gypsum rock panels separated by air.

Permittivity: Constant of proportionality that exists between electric displacement and electric field intensity, it is specified relative to free space permittivity ($\epsilon_0 = 8.854$x1012).

Conductivity [S/m]: Measure of the ability of a given material to transfer electric charge or heat, equal to the reciprocal of the resistance.

Thickness [m]: Several material types use also thickness as parameter in the formulas to determine reflection and transmission coefficients as explained in section 2.2.3.

The main goal was to simulate the presence of people trapped in the building so I initially chose points, the simplest kind of transmitter and receiver.
I settled the transmitters at each floor randomly distributed but still trying to get a layout as uniform as possible in order to cover every corner of the building and considering that each component can be locate independently.
After that I placed two receivers points (reproducing the air-drones) at 20m height and at a distance of about 5m from the external walls, one roughly in the middle on the longest side of the building and the other centrally located on the shortest side to distinguish the differentiation in the two cases.
The intent was to determine whether there can be a close dependency between outputs and locations and if the peculiar positioning of the destinations along the building impacts the values of the measurements and and therefore the obtained results.

Transmitter and receiver points can be assembled in sets where all the elements share the same properties like, for example:

- Coordinate system (cartesian, longitude/latitude and UTM)
- Antenna (model, gain, polarization etc)
- Waveform (signal radiated from antenna's properties like type, frequency and bandwidth)
- Input power

3.5.1 Coordinate System

The definition of the Coordinate System is a crucial aspect as it affects not only the measurement's results but also how we display and read data but, above all, the results. The angles considered during the computation, first of the electric field and then of all the other outputs, are specified in terms of the spherical components at the transmitter or receiver point using a polar coordinate system, shown in Figure 3.7 (a).

$$\begin{cases} x = \rho \sin\phi \cos\theta & \rho \in [0, +\infty) \\ y = \rho \sin\phi \sin\theta & \phi \in [0, \pi) \\ z = \rho \cos\phi & \theta \in [0, \pi) \end{cases} \tag{3.7}$$

ϕ is the *Azimuth*: angle between the positive x-axis and the line segment from the origin to the projection of the point considered on the xy-plane.
θ is the *Zenital Distance*: angle between the positive z-axis and the line segment from the origin to the point considered.
So for instance, considering this coordinate system, it is possible to determine the direction from which the wave reaches the receiver or towards which it is directed from the transmitter (*Direction of Arrival* and *Direction of Departure*).

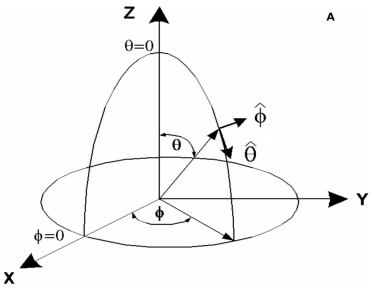

Figure 3.6: Spherical coordinate system.

At the beginning the origin of Cartesian coordinate system was placed exactly at floor level in the center of the building and the position of each element was assigned according to this reference system.
I then decided to realize a roto-translation of the original system in order to obtain the desired outputs with respect to our points of interest (receivers). So, concerning to achieve that, I first made a rigid translation to set the standpoint in correspondence of the receivers leaving the orientation of the axes unchanged.
Considering a generic point $P = (P_x, P_y, P_z)$, to get the coordinates translated w.r.t $R_1 = (R_{1x}, R_{1y}, R_{1z})$ and $R_2 = (R_{2x}, R_{2y}, R_{2z})$ these relationships are worth:

$$P' = \begin{cases} P'_x = P_x - R_{1x} \\ P'_y = P_y - R_{1y} \\ P'_z = P_z - R_{1z} \end{cases} \qquad P'' = \begin{cases} P''_x = P_x - R_{2x} \\ P''_y = P_y - R_{2y} \\ P''_z = P_z - R_{2z} \end{cases} \tag{3.8}$$

In second step I rotated by the angles θ and ϕ founded considering the LoS path direction of arrival, identified by each transmitter, as reference.
In order to to do this I introduced the rotation matrices, first rotating by ϕ compared to Z-axis then moving by θ compared to Y-axis.

$$R_z(\phi) = \begin{bmatrix} \cos\phi & -\sin\phi & 0 \\ \sin\phi & \cos\phi & 0 \\ 0 & 0 & 1 \end{bmatrix} \quad R_y(\theta) = \begin{bmatrix} \cos\theta & 0 & \sin\theta \\ 0 & 1 & 0 \\ -\sin\theta & 0 & \cos\theta \end{bmatrix} \tag{3.9}$$

Considering 3.8, we obtain:

$$P'_{rotat} = R_y(\theta)R_z(\phi)P' \qquad \text{and} \qquad P''_{rotat} = R_y(\theta)R_z(\phi)P''$$

In this way, as we can see in Figure 3.7, we get the exact overlap of the Z-axis on the trajectory identified by the LoS path of each transmission and

we have the possibility to better understand the distribution of the angles with respect to the LoS ideal segment.
To prove that I've got the right transformation, representing the coordinates of each transmitter, we realize $(0, 0, d(receiver, transmitter))$ to which correctly correspond $\theta = 0 \quad \phi = NaN$.

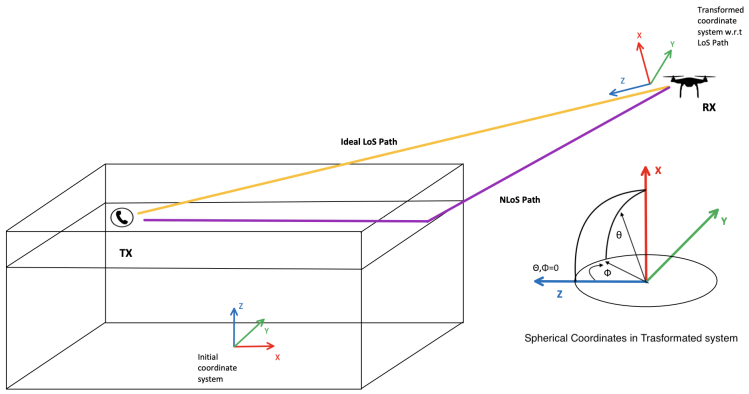

Figure 3.7: Transformed coordinate system.

3.5.2 Settings

Waveform	*Type*	*Frequency*	*Bandwidth*
	Sinusoidal	1.8 GHz	10 MHz
Antenna	*Type*	*Polarization*	*VSWR*
	Isotropic	Horizontal	1.000

Table 3.2: Properties.

Isotropic Antenna

Known also as *Omnidirectional* or *Unipole* it is an ideal component frequently used as theoretical reference in comparing different practical radiating types

of antennas and simplify range estimation analysis.
Its peculiarity is that it is able to emit a spherical shaped signal and detect the signal uniformly in all directions, this means that in any orientation the transmitted signal power is the same.
On the other side, in a real *Directional* antenna, radiated power is a function of the angle and in some paths it is stronger than in other directions.
In other words by orienting appropriately the central beam the purpose is to improve transmission and reception communications, reducing interference w.r.t an equivalent omnidirectional antenna.

Frequency Band

As the years go by we are observing a continuous expansion of the frequency spectrum with the progressive shift to higher bands that, while ensuring less crowding, they guarantee a lower degree of penetrability and they are therefore more attenuated in propagation through physical medium different from air or blocked due to the presence of obstacles.
As a matter of fact, waves penetrability depends on the material's resistivity and permittivity but it is also limited by a parameter called *Skin Depth*.
It is defined as the depth at which the density of the electric field has decayed to $\frac{1}{e}$ (about 37%) of the value at the surface and it is inversely proportional to the decay constant:

$$\delta = \frac{1}{\beta} = \sqrt{\frac{\rho}{f\pi\mu}} \tag{3.10}$$

As we can see it is inversely proportional to the frequency and, thanks to the ρ parameter, it is conditioned by the physical properties of the media.
That's why each frequency level is less or more appropriate depending on the propagation environments, for example, low frequency (450 MHz) is suitable for countryside coverage, GSM 900 (900 MHz) is used for light urban coverage and high frequency (1800 MHz) presents disadvantage when we take into account dense urban coverage for the reason cited so far, but it is a decided

advantage when it comes to capacity.
Today the majority of phones support the use of multiple bands and also multi-mode.
In our setting, in order to consider the limitations given by structural walls, I have chosen to use 1800 MHz band (DCS 1800), an upbanded version of GSM that allows the use of mobile phones with additional services such as data transmission and internet connection.

Polarization

The orientation of electric field vector establish the antenna polarization, this is an important factor to be considered during the design step before assemble radio antennas or even integrate them into wireless or mobile communications systems. There are several categories of polarization which, in turn, are divided into subcategories each one with its merits, defects and preferred usage environments.
The three main groups are *Linear polarisation*, *Circular Polarization* and *Mixed polarisation*, I will only take into account the first one, that is the most common for antennas and it is characterized by the fact that all of the radiation lies one plane. On the other side Circular one is mostly used for satellite implementations and Mixed (known also as elliptical polarization) is an hybrid formed by the union of the first two.
The two linear polarization's subclass are *Vertical* and *Horizontal* distribution, I chose the first one, where electric field vector of electromagnetic wave is oriented parallel to the earth because it guarantees a good angle of radiation in opposition with the lower one owned by the vertical polarization that enable a large part of the power to be radiated at an angle close to the earth's surface.
A crucial point is the polarization matching of the RF antenna with the incoming signal ones in order to get the maximum signal obtainable.

VSWR

Known as *Voltage Standing Wave Ratio* is defined as the ratio of the maximum to minimum voltage on a transmission line structure.
It is important to deal with this term during the configuration phase as it is an indicator of the power amount that is not accepted by the antenna and therefore is reflected back along the transmission line.
So, for this reason, it is a function of the reflection coefficient (also known as return loss) and it is defined as follow:

$$VSWR = \frac{1 + |\Gamma|}{1 - |\Gamma|} \tag{3.11}$$

Smaller the VSWR is, better the antenna is matched to the transmission line and more power is delivered to the antenna.
The perfect match is given by 1.0, which is the ideal case considered by us, in fact in this condition no power is reflected back from the antenna.

I set waveform's and antenna's properties associated (shown in Table 3.2) the same both for sources and destinations in order to semplify the analysis, the model setup and speed up the calculation.

Chapter 4

Wireless Insite Ray-tracing Simulation Software

This chapter describes the analysis of the scenario we implemented through the use of Wireless InSite [13]. First, a brief introduction about the program, the models adopted and their peculiarities and then the description of the outputs request.
Before to proceed through the transmission computation in the structure built we wanted to guarantee a sufficient level of stability to the results of the simulations but above all to the analysis of the data conducted in post-processing.

4.1 Wireless Insite Settings

4.1.1 Study Areas

A Study area defines three important aspects that profoundly influence the results of simulations and also give the possibility to optimize the computation time taken:

- Region of the project in which conduct the analysis.
- Propagation model to be used in calculating the power transferred from Transmitters to Receivers within the study area.
- Set of outputs to generate during the simulation.

Many different study areas can be built in a project, each one with own peculiarities as different dimensions, independent propagation model and parameters. Thanks to this possibility, results from various calculation can be compared and more than one simulation can be carried out at the same time in parallel, exploiting in this way the maximum available computer resources (GPU) reducing the computation time taken.
Elements which fall outside the study area boundary are not considered.

Properties and Model Input Parameters

Ray Spacing: The spatial separation between rays shot from transmitters used to evaluate the electric field strength

Reflections: Indicates the maximum number of reflections which a path can undergo

Transmissions: Indicates the maximum number of transmissions which a non-diffracted path can undergo

Diffractions: Indicates the maximum number of diffractions which a path can undergo

After the definition of Study Area's characteristic, each ray-based model allows the user to select which output files will be generated during simulation such as electric and magnetic field strength, received power, interference measures, path loss, delay spread and many more.

Wireless InSite [13] provides several ray-based propagation models, they are

all used to find the propagation path between each transmitter and receiver points through the project's urban geometry implemented.
Each model can be more or less suitable depending on the situation considered but especially connected to the accuracy of the desired outputs with the resources available. The majority includes the effects of reflections, transmissions, and diffractions on the electric field but only X3D and FULL 3D models allow transmissions through building walls so we focus out attention considering in particular these two configurations.

We've initially examined FULL 3D model in our simulation, first because it is the legacy model, and the other reason is that it allows compatibility also with older projects permitting each kind of interaction with no restriction on object shape.
This capability is important in our environment where propagation paths with transmissions through walls were considered to model propagation in indoor environments but also in scenarios obtained by a combination of indoor and outdoor components.

4.1.2 X3D Model

Later on we've changed performing the same analysis using the last outcome of the software improvement. Indeed X3D is an advancement with respect to previous models, it has been developed with the goal to provide an highly accurate raytracing scheme taking advantage of multi-core processors.
It offers many benefits like the speed-ups acquired with the GPU acceleration and multithreading, and the accuracy reached through the exact path calculations.
Wireless InSite's X3D model also provides features like diffuse scattering, atmospheric absorption and MIMO antennas available.
A more detailed description of each model can be found on the Reference Manual [13] in the chapter dedicated to Propagation Models (chap.16).

X3D SBR ray tracing algorithm is similar to the one described in general (see section 3.3) and suitable for full3d with some differencies:

- X3D ignore the single-sided versus double-sided property of a face.
- After finding the paths, it implements an Exact Path Calculator (EPC) algorithm. EPC is meant to adapt the interaction points (reflections, diffractions and transmissions) so that paths end at the exact receiver location reducing the presence of errors in power calculation. It also verifies that the correct path is not hampered by any face and all of the diffraction and reflection angles are valid. Paths that fail this verification are discarded.

Diffuse scattering: It is the stochastic process for which scattered paths are caused by inherent irregularities in real-world structures and materials, the model used by X3D to simulate this situation is based on the results of Degli-Esposti's studies. Its contribution is not limited to the specular direction but on the contrary can therefore results in paths oriented to any direction that can reach the receiver point provoking a large increase in the potential propagation paths between transmitters and destinations and giving a variant of received power output.
The fraction of reflected power that is scattered diffusely from a surface rather than reflecting in the standard direction is defined through the diffuse scattering coefficient, S, given by:

$$S = \frac{|\vec{E_S}|}{|\vec{E_i}|} \tag{4.1}$$

where E_S is the diffuse scattered field and E_i is the incident electric field.

Atmospheric absorption: It's a frequency dependent absorption caused by oxygen and water content in the atmosphere according to wavelength. Total attenuation is the sum of 4 Terms: Free space path loss, attenuation caused by oxygen absorption, attenuation caused by water vapor absorption and Rain attenuation, when present.

$$Atten_{Total} = Atten_{FreeSpacePathLoss} + Atten_{Oxygen} + Atten_{WaterVapor} + Atten_{Rain}$$

Users can indicate the humidity, temperature and pressure to get highly efficient prediction.

MIMO: This use of multiple antenna system has been developed with the objective of increasing the performance potential at the physical layer.
In a wireless system a MIMO architecture is characterized by N antennas at the transmitter and M at the receiver and we can distinguish among three important families of solutions: *Diversity, Spatial multiplexing* and *Beamforming*.
This structure is supported in Wireless InSite that guarantees all the tools necessary to create arrays.

4.2 Outputs

Electric Field Evaluation

The starting point to extrapolate then all the other outputs is to find the electric fields in the far zone of the transmitting antenna.
They are evaluated in the same manner both for FULL 3D and X3D and in free space in the direction (θ,ϕ) at a distance r can be written as:

$$E(r,\theta,\phi) = (A_\theta(\theta,\phi)\hat{e}_\theta + A_\phi(\theta,\phi)\hat{e}_\phi)\frac{e^{-jr\beta}}{r} \tag{4.2}$$

$$A_\theta(\theta,\phi) = \sqrt{\frac{P_T\eta_0}{2\pi}}g_\theta(\theta,\phi) \tag{4.3}$$

$$A_\phi(\theta,\phi) = \sqrt{\frac{P_T\eta_0}{2\pi}}g_\phi(\theta,\phi) \tag{4.4}$$

P_T is the time-averaged power radiated by the transmitter
$g_\phi(\theta,\phi), g_\theta(\theta,\phi)$ are the θ and ϕ components of the gain of the transmitting antenna in the spherical coordinate system (3.7).

Received Power

The time averaged Received power is calculated through a coherent sum (with phase) of the quantities from each path to the receiver

$$P_R = \sum_{i=1}^{N_P} P_i \tag{4.5}$$

N_P is the number of paths
P_i is the time averaged power in watts of the i^{th} path and is given by:

$$P_i = \frac{\lambda^2\beta}{8\pi\eta_0}|E_{\theta,i}g_\theta(\theta_i,\phi_i) + E_{\phi,i}g_\phi(\theta_i,\phi_i)|^2 \tag{4.6}$$

θ_i and ϕ_i give the direction of arrival.
Once the received power in watts is found, the power in dBm is determined from:

$$P_R(dBm) = 10\log_{10}[P_R(W)] + 30dB - L_S(dB) \tag{4.7}$$

L_S is the additional loss in the system which can be stated through the cable loss field.

Propagation Paths

It consists of the geometrical ray paths through the ambiance from the transmitter to the receiver, in this way all the forms of interactions (usually reflection, transmission or diffraction if no foliage surfaces are present) that each ray undergoes are shown.
The interplay undergone by each path are saved in sequence form in a list of the interaction designations:

Interactions	**X3D**	**Full 3D**
Transmitter	Tx	Tx
Receiver	Rx	Rx
Reflection	R	R
Ground Bounce	R	G
Transmission	T	T
Diffraction	D	D or d*
Enter/leave foliage	F/X	F/X
Diffuse Scattering	DS	-

Table 4.1: Propagation Path Interactions.

Path Loss and Excess Path Loss

$$L_{PL}(dB) = P_T(dBm) - P_R(dbM) + G_T(dBi) + G_R(dBi) - L_S(dB) \quad (4.8)$$

Path gain is equivalent to *Path loss* (even if it is less common) and it is expressed with the opposite sign.
Excess Path Loss is an additional losses usually caused by the urban environment

$$L_X(dB) = L_{PL}(dB) - L_{FS}(dB) \quad (4.9)$$

L_{FS} is free space loss with or without the antenna patterns.

Angle of Arrival

It is one of the information with distance, time-of-arrival and direction of departure obtainable through the evaluation of ray path. It is the orientation in spherical coordinates from which the propagation path arrives at detection device.
As we have explained in 3.5.1, we modify the initial coordinate system to get a transformed one where the angles of the direction of arrival are given w.r.t the ideal LoS trajectory, for this reason θ and ϕ are estimated referring to the Z axis.

$$\theta = \frac{\pi}{2} - \arccos \frac{x}{\sqrt{x^2 + y^2 + z^2}} \quad (4.10)$$

$$\begin{cases} \phi = \pi & y = 0, z < 0 \\ \phi = 0 & y = 0, z > 0 \\ \phi = -\frac{\pi}{2} - \arctan(\frac{z}{y}) & y > 0, z > 0 \\ \phi = -\frac{3\pi}{2} - \arctan(\frac{z}{y}) & y > 0, z < 0 \\ \phi = -\frac{\pi}{2} - \arctan(\frac{z}{y}) & else \end{cases} \quad (4.11)$$

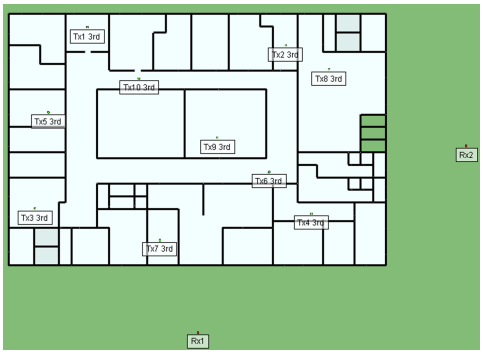

Figure 4.1: Random Transmitters Deployment.

4.2.1 Results stability

Before the disposition of the whole transmitters, we took an intermediate step in which we selected a subset of 10 transmitters picked randomly at each floor. We've done several tests, changing not only the coefficients values but also the simulation model applied, to set the study analysis parameters in order to see the differences and discard the less reasonables.
In fact the estimation accuracy can be enhanced by increasing the number of reflections, diffractions, or penetrations but this must be done keeping in mind the objective of choosing the most likely condition and of assessing the stability of simulations.

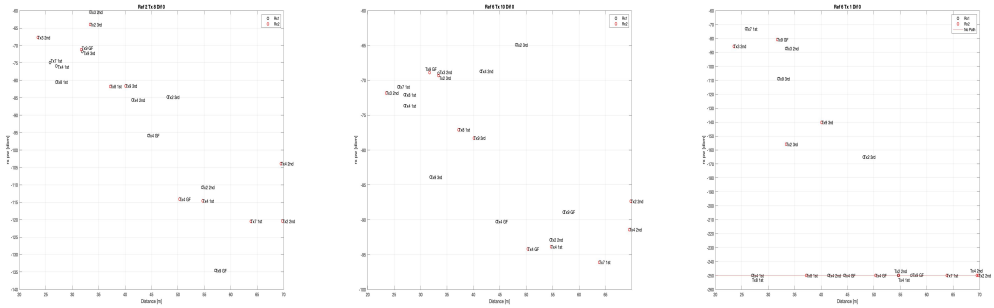

Figure 4.2: Example of different results changing parameters for 10Tx.

At the beginning, how we could have expected, the values obtained with each simulation were very different from each other, but once we passed from FULL3D model to X3D we reached the most stable results reducing considerably the calculation time.

Chapter 5

Numerical Results

In this chapter we present the Data Analysis done after the realization of the whole structure. I proceed placing an array of 100 transmitters for each floor collecting a total of 400, setting the transmitters' height so as to differentiate seated individuals by those standing or walking on the stairs.
After carrying out the simulation phase and have obtained a sufficient number of measures I switched to the data analysis and to the organization of these in order to perform curve models that gave us precise indications of the obtained results.

5.1 The Impact of Distance

The first discretization parameter I take into account is the pure distance [m] calculated throught the ray tracing analysis.
The main difference between the results is given by the discrepant positioning of the two receivers, in fact, as explained in (3.5), RX2 is located in correspondence of the shorter side of the building and for this reason performs averages longer distances than RX1 (as shown in Table 5.1).
One of the main purposes of our work is to highlight and evaluate the varia-

tions between receiver placements with the aim of determining whether one of the two is better in terms of coverage, received power and direction of arrival.

Floor	**RX1[m]**	**RX2[m]**	**Difference**
Ground	40,700	48,316	+15,8 %
1st	38,414	46,047	+16,6 %
2nd	34,872	41,097	+15,1%
3rd	30,880	39,699	+22,2 %

Table 5.1: Distances average.

The discrepancy between the depth of the building in each of the two cases plays a key role in the evaluation of the outputs for all the floors.

5.2 Curve Fitting

Curve fitting is one of the most powerful and widely used tool for data visualization in the Data Analysis, it has the goal to design a curve which defines a "best fit" model of the relationship between one or more predictors (independent variables, assumed to be the result of an exact measurement process without random error) and a response variable (dependent variable measured with random error) [14].
When their dependency is reasonably approximated by a straight line, we talk about *linear regression*, if instead the relationship follows a curve, we call it *curvilinear regression* but there is also the case in which the starting values are not linear named *non-linear regression* models.
Linear models are preferred with respect to non-linear ones because of linear models are mathematically easier to work with. On the contrary, nonlinear

models must use iterative schemes that may gather several solutions.
For this reason, the first solution is a good starting point to find the desired relationship and approximation and it is the one I used.

I begun our regression analysis using a linear customed equation derived by a combinations of a set of basis functions and applying it on the transmitters distance.
A and B are the parameters, which are known constants linking the two variables, B is the y-intercept and A is the slope. I used log-normal path-loss model as a generalization of the free-space Friis equation where the power is allowed to decrease at a rate of $(1/x)^n$ and a random variable is added to take into account additional effects.

$$y = A * f(x) + B \qquad y = A * (-10m \log(x)) + B \tag{5.1}$$

x is the array distance between transmitter and receiver extrapolated from the simulations, m is the path loss exponent (see 3.1), which varies between 2 for free space up to 6 for indoor building propagation.
The values assumed by A and B are slightly different depending on the receiver considered.

Results	**RX1**	**RX2**
A m=2	2.624	2.656
A m=3	1.75	1.771
A m=6	0.8748	0.8854
B	103.9	108.3
SSE	1.145e+05	1.11e+05
R-square	0.4193	0.5521
RMSE	16.96	16.7

Table 5.2: Curve fitting Coefficients

Sum of squared estimate of errors (SSE): sum of the squared differences between each observed value and the value estimated by the regression line (its group's mean) and can be used as a measure of variation within a cluster. Indeed it is an indicator that a good regression has been reached: a low value indicates that the regression model can better explain the data while a higher SSE indicates that the model poorly explains the data.

R-square: known as the coefficient of determination, it weigh the scatter of the data points around the fitted regression line and it is always a value between 0 and 100 %. Higher is the percentage, better the regression model fits the observations.

Root Mean Square Error (RMSE): RMSE is a measure of the spread of the y values around that average, it is used to evaluate accuracy for continuous variables and the average magnitude of the error. Mathematically it is given by the square root of the average of squared differences between prediction and actual observation.

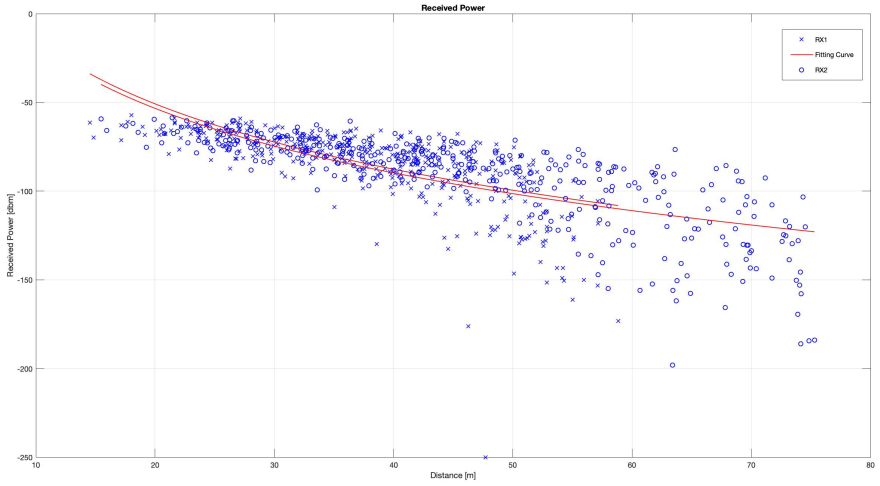

Figure 5.1: Received Power vs Distance

The direct observation of the curve w.r.t the transmitters position (and hence the distance), but more specifically the value assumed by the parameters cited so far used to test the accuracy of the fitting curve, told us that the received power trend follows a similar tendency following a constant decay up to the distance of about 35m, after which a more rapid lowering occurs, for this reason an approximation of the regression through a broken line would have been more representative for the situation under our consideration.

5.3 Receiver Sensitivity

Another key parameter that has a strong influence on the performance of any radio communications system is the *Radio Receiver Sensitivity*.
It is defined as the lowest received signal power at which the node is able to accurately decode a given signal and clearly receive the bits that have been transmitted achieving a certain Bit error rate (BER) performance.
It is measured in dBm and narrowed by external noise interference that can be induced by many variety of sources, be generated within the radio receiver or acquired externally by the antenna.
As a result, during the design of the system, the evaluation of noise optimization is an essential step to guarantee satisfactory performance of the whole radio receiver, indeed it is important to be conscious that all of the noise sources are dependent on frequency and their effects can be relevant or not depending on the bands used by the specific communication system.
This performance parameter can also be expressed in relation to other figures of merit [15] that are more useful in a telecommunication application context like:

- *Signal to noise ratio (SNR)*: compares the power level of a desired signal to the undesired noise within the system
- *Bit error rate*: proportion of bit errors relative to the total number of

bits transferred during a specific time interval.

- *Noise factor/Noise figure*: measure of degradation of the signal to noise ratio in a device caused by the noise added by a unit.

A typical range for receiver sensitivity for RF modules is below -50 to -100 dBm, more in details, as specified in [16], receiver sensitivity of a common 802.11g modulation standard product that works in the 2.4 GHz band is -85 dBm, on the other hand, on average Wireless products on the market have -105 dBm, values that doubles every time the transmit power is increased by 3 dB. Professional equipment provide up to -120 dBm but in modern HF receivers values up to -135/-140 dBm can be reached.
I am going to assume -85 dBm as reference value in order to figure out the received power percentage above and below the threshold given by this sensitivity value. The choice of this value is motivated by the fact that 802.11g version is commonly used to provide wireless connectivity in the home, office and some commercial establishments.

5.4 Received Power Distribution

In the representation of the power contributes density distribution obtained for both Receivers, in order to present a delineation as intuitive as possible, I divide the Received Power into bands that roughly coincided with the sensitivity levels of the the most commonly used receivers, in the range below -65 to -135 dBm.
The received signals that have values below -135, value taken as lower limit, have not been included both in the graphic representation and in the density calculation as it has been established that for values below this limit the signal received is 0.
As we have observed so far (sects (2.3) and (3.5) in *Characteristics of used materials*), a decisive role is played from electromagnetic interaction of the

materials crossed during signal propagation that cause a substantial attenuation and severe diffraction loss, indeed in a so complex location pure distance is an interesting parameter which must be contemplate and it is closely connected with the number of obstacles interaction, but it's not enough to give us a useful indication if considered alone.

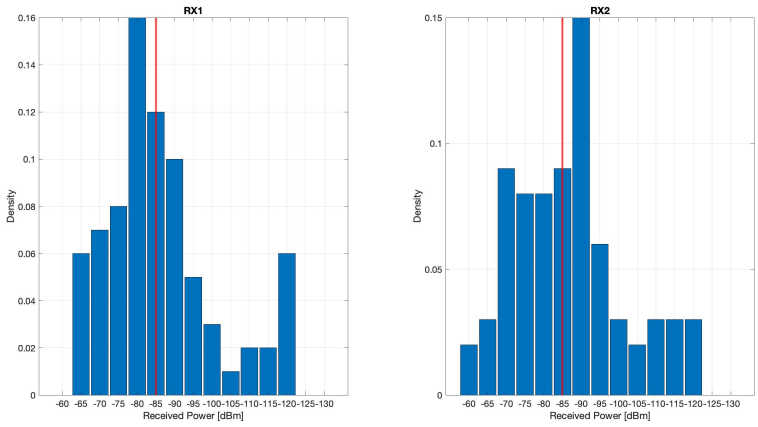

Figure 5.2: Received Power Distribution Ground Floor.

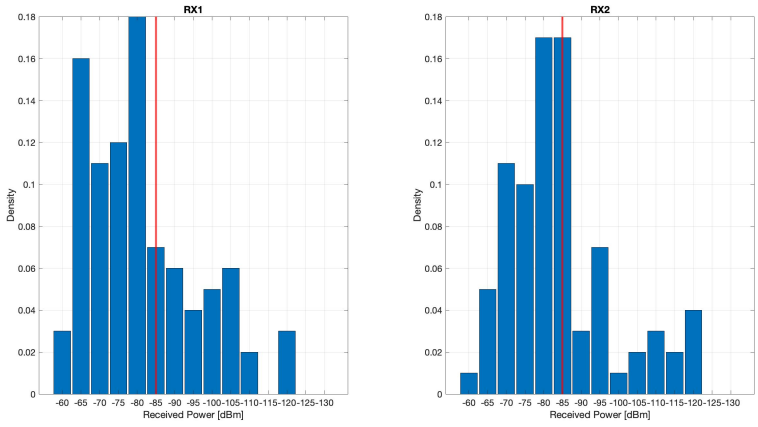

Figure 5.3: Received Power Distribution 1st Floor.

The data representation, obtained with regard to the received power density considering the transmitters placed in the ground and first floor of the struc-

ture, confirms what has been supposed. In fact watching the ground floor and considering separately the two receivers, 47,4% of the received power settles above the reference value as regards RX1 and the value drops further at 40,5% for RX2. The trend slightly improves going to the upper floor, in this case the values grow respectively to the 64,5% and the 53%.
Although a fairly homogeneous density profile was obtained, there is a thickening of the power values for values exceeding the lower bound -135 dBm in both floors (22% and 26% of the total at Ground Floor, 7% and 17% at First Floor) from which it is easy to understand that this is induced by the increase of the attenuation value because of the greater distances traveled by the signal with the consequent higher number of interactions and crossed surfaces (measurements were taken with all windows and doors closed).
As we have seen and has been studied in previous works [17], the three main agents that attenuate the signal strength of any system and affect the overall performance of the cellular network signal inside a building are *Reflection*, *Diffraction* and *Scattering*, the combination of which causes Multipath fading (3.1).
In particular, reflection factor increases proportionally to the length of the path and to the dimensions of the obstacles with respect to the wavelength of the signal treated.
For this reason this component is often dominant in indoor application while it loses its relevance in outdoor environments.

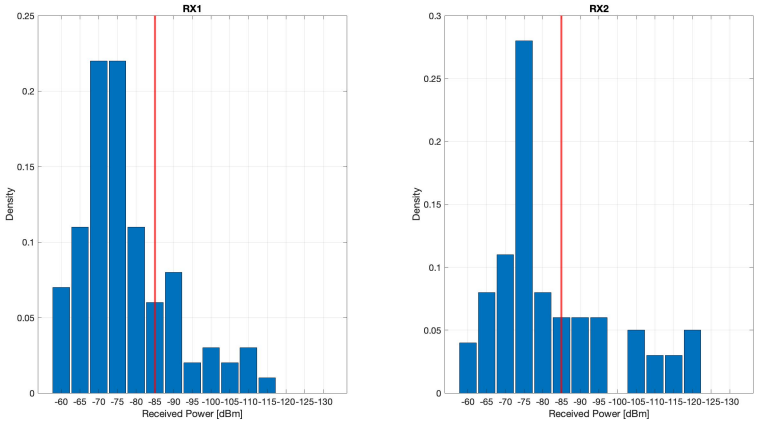

Figure 5.4: Received Power Distribution 2nd Floor.

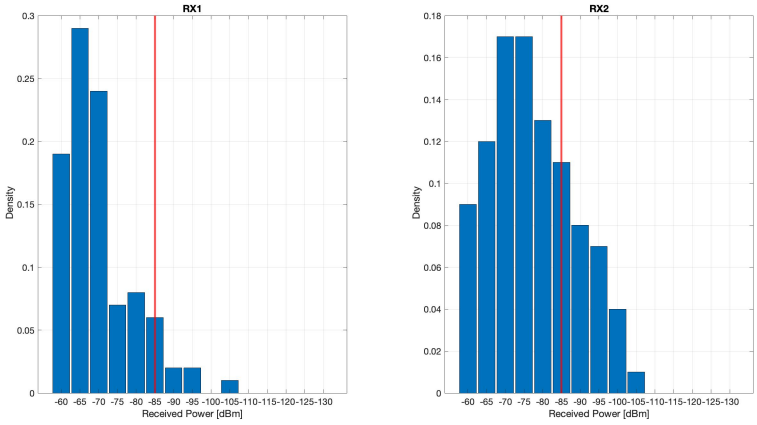

Figure 5.5: Received Power Distribution 3rd Floor.

Moving on to the results obtained with regard to the second and third floors, it can be noticed that, together with the consequent approach between transmitters and receivers, there is a clear migration from negative received peaks power values that exceeded the limit, towards outputs included in the band between -65 and -85 dBm in which we find the highest density. The percentages comes to aid to confirm this tendency since for second floor the 74,5% and 63,4% of received signals by RX1 and RX2 are above -85 dBm and as

far as last floor (3rd) values rise further reaching the 88,8% and 68,7%.
As a direct consequence of this there's a noticeable reduction of signals that are not being received that settles down at 2% and 7% and at 2% and 1% of the total respectively referring to RX1 and RX2 for the two levels.

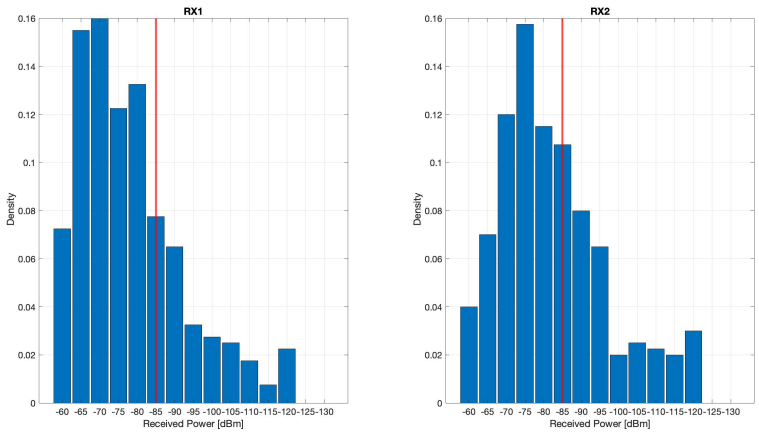

Figure 5.6: Received Power Distribution Total Building.

The received power density distribution for the whole building realized combining the extrapolated data for each floor, demostrates how the trend of the total received power levels follows a similar tendency showing a higher density in the bands between -65 and -85 dBm (as we have seen for 2nd and 3rd floor), confirmed again by the proportions: 70 % for RX1 and 57,5 % for RX2 are above -85 dBm.
As estimated the positioning of the receivers affects significantly the results going to reduce consistently the density of values beyond our limit, that in the Total evaluation is at 8,25 % and 12,75 % .
An useful overview is given by the Table 5.2 that provides a summary of what we've said so far with the help of bar charts.
The ratio estimated for values falling below the lower limit it is calculated with respect to the total amount.

Floor	$>$ **-85 [dBm]**	$\leq$ **-85 [dBm]**
Ground RX1	47,4 %	52,6 %
Ground RX2	40,5 %	59,5 %
1st RX1	64,5 %	35,5 %
1st RX2	53 %	47 %
2nd RX1	74,5 %	25,5 %
2nd RX2	63,4 %	36,6 %
3rd RX1	88,8 %	11,2 %
3rd RX2	68,7 %	31,3 %
Total RX1	70 %	30 %
Total RX2	57,5 %	42,5 %

Table 5.3: Received Power percentage w.r.t receiver sensitivity.

5.5 Direction of Arrival

Another interesting evaluation can be carried out considering the distribution of the directions of arrival obtained through the ray path analysis of the signals emitted by each transmitter (4.2).
In practice, as explained in [18], the computation is a tough issue, made difficult by the fact that there are usually an unknown number of signals involved, each one from unknown directions and with unknown amplitudes and it needs precise synchronization amongst pattern elements.
This estimation could have many large-scale applications and opportunities of evolution with, for example, the future appliance of the achieved results especially in post-disaster complex propagation conditions like the one I am considering. As a matter of fact it can be used to localize targets and people trapped in the edifice who need to communicate with the rescue units but not only, actuality the demand for accurate localization is growing rapidly despite the difficulty in obtaining positional information from the received waveforms especially in harsh wireless propagation environments.
Localization-of-Things (LoT) is the field that deals with process of locating any possible collaborative or non collaborative nodes extracting their positional informations as meticulously explained in [19].
The precision of conventional localization techniques depends heavily on the quality of single-value estimates (SVEs) determined from inter- or intra-node measurements. It is necessary to obtain measures that are as precise as possible and, because of this, the accuracy of SVE-based localization techniques degrade in wireless environments due to biases caused by multipath propagation and NLOS conditions.
To take a decisive step towards the localization performance improvement, it is essential to design networks that exploit soft information (SI), such as techniques that rely on a set of possible values rather than on single distance estimates (SRI) together with the use of environmental information, such as contextual data.

After the transformation of the coordinate system (translation+rotation) and the transition of the reference system regarding the calculation of the arrival angles in spherical coordinates, I proceed to the representation of them in figures that show us the general trend through the use of Matlab.
To obtain that I consider in my investigation a set of 25 paths acquired by the receivers from each transmitter, taking as indicator points $P = (x, y, z)$ used to perform the polar computation, the last interaction between the propagation path and the building before reaching the destination.
These are defined, in almost all cases, by the specific position where the signal cross through the outer wall or, in the case of the top floor, straight to the rooftop.
In the following charts I reproduce the θ (red mark) and ϕ (black circle) component of the 25 points of interest acquired through propagation paths received by RX1 and RX2 from 60 Transmitters at 3rd floor.

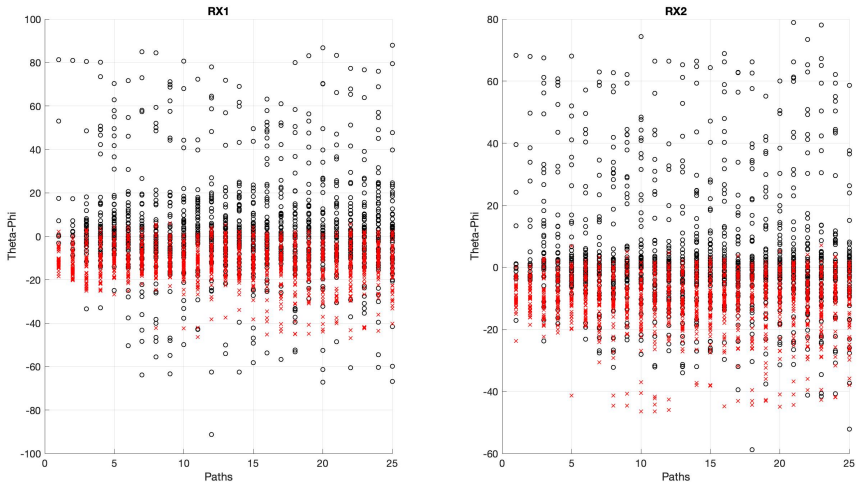

Figure 5.7: Theta and Phi Direction of arrival 3rd Floor.

Explaining this representation more in details, we can see how in the two receivers θ values are predominantly accumulated around zero but, more in general, they assumes both positive and negative amount (all values are included within a range that goes from -50 to 6/7 degrees) with a clear

preponderance of negative attitude given by the positioning of the receivers, which are disposed significantly higher than the transmitters and the rest of the structure. For this reason, in fact, confirming the results obtained, almost all the rays received come from below the LoS trajectory which is taken as reference, the few joints from slightly above are the result of exceptional signal reflections but they are a clear minority.
The progression of θ values is specular for both RX1 and RX2 because the positioning in correspondence of two different sides of the building does not affect the measurements but, in this case, the key component is the height with respect to the ground which is the same for both.
On the other hand, if we take into account ϕ, the trend undergoes a discreet change. Also in this case, in fact, the majority of the values found are around 0 and the angles assume negative and positive values dictated by the arrival of the rays both from "right and left" of the LoS reference trajectory, but variance is much wider since the transmissions through the walls, but above all the reflections, cause a widening of the arrival angle width.
Differently from what we said for θ, ϕ results change according to whether we consider RX1 or RX2, in fact the peculiar length of one side of the building with respect to the other one becomes an important element during the transmitter deployments and consequently the simulation.
The main discrepancy can be seen since ϕ takes values included in the range between -90 and +90 degree being RX1 precisely located in the middle on the "longest" side and for this reason receiving paths with wider angles, while it takes values in the shorter range between -60 and +80 degree being RX2 facing the shortest side.

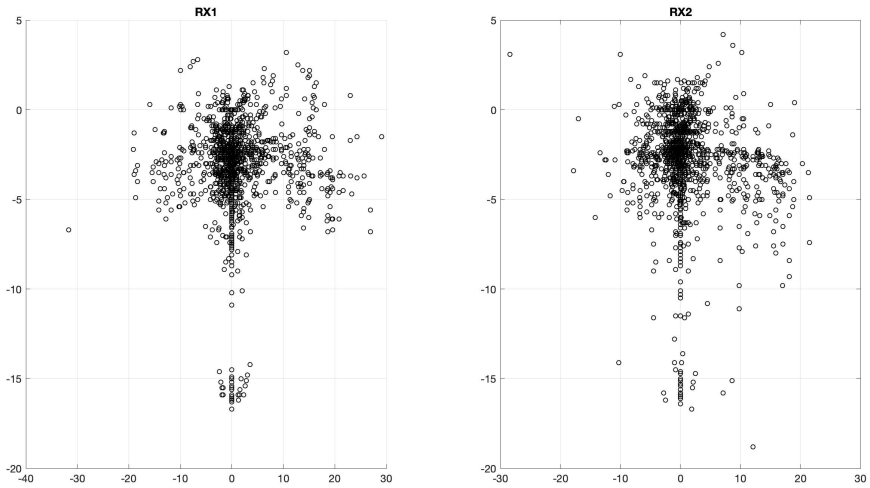

Figure 5.8: X and Y Direction of arrival.

In this diagram (Figure 5.6), I placed the observer at the correspondence of the two receivers lying on the plane parallel to the one containing the LoS direction, with the aim of making the directions of arrival detection even more intuitive. In this image the origin (0,0) coincides with the reference trajectory and the set of marks shows the orientation of the arrival in X and Y coordinates leaving apart the Z ones which indicates the depth.
This is done with the objective to certify what was already been said about the arrival directions analyzing the previous plot.

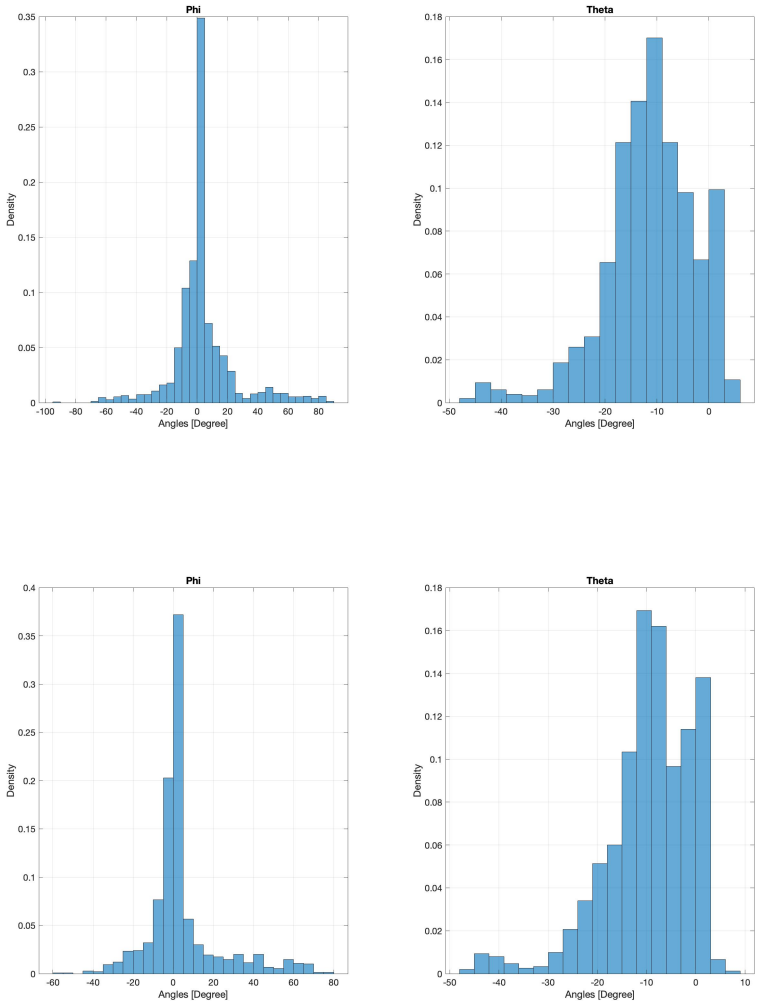

Figure 5.9: Probability Density Theta-Phi Rx1 and Rx2.

These last graphs have been performed throught "histogram" Matlab function that, if applied to the array of the elements, it produces a discrete probability density function along the x-axis between the minimum and maximum values assumed by the vector.
Also thank to them, the analysis I made has been confirmed, proving what we said about the trend of the arrival angles for both receivers.
They help to further emphasize first the fact that for both receivers most of the ϕ values are concentrated around 0 degree and a considerable higher

variance is present, and on the other side, for what concern θ, to better appreciate that angles mainly assume negative values seemingly because of paths arrival directions which, in almost all cases, arrive below the reference LoS direction.

Chapter 6

Conclusions and Future work

The aim of this thesis was the channel characterization of an air-to-ground link in an Indoor-to-Outdoor Scenario, where mobile terminals inside a building towards outdoor unmanned aerial vehicles (UAV) or drone, with mini base station on board.
A special focus has been dedicated to received power and directions of arrival evaluations to explore how the density distributions changes according to the floor taken into consideration keeping the UAV at a fixed height.
As far as the received power is concerned a clear behaviour has been found. Specifically, I experimented a progressive increase in the power density concentration in the range above -85 dBm (chosen as reference considering the sensitivity of receivers that apply 802.11g modulation standard) starting from the ground and proceeding to the upper floors.
In the construction environment phase I built a 4-storey parallelopiped building 16 meters high, the longest side of 60 meters and the shortest side of 40. I placed two receivers 20 meters high, one positioned approximately in the center of the long side and the other in the center of the short side with the goal to evaluate the differences between the results given by the two.
Considering what I have found in my work, supported by the simulations outputs, we can claim that the received power levels follow a similar trend

for both receivers, showing a density increase in the bands between -65 and -85 dBm when we gradually proceed from the ground floor towards the transmitters reducing the distance and therefore the possible signal interactions with the structure. So, from this fact, we can understand that the receivers' positions regarding the sides of the building is not the parameter that affects the received power attenuation, which is instead more influenced by the altitude of UAV.

As a result of my analysis, and thanks to the flexibility of the UAV movement, we may expect that considerable improvements can be obtained and the attenuation can be reduced, by choosing to move the UAV progressively from the terrain up to the rooftop (or viceversa), compared to the situation where it remains fixed at a predefined height (considered in this work).

Regarding the direction of arrivals analysis performed using the ray-tracing technique, the angles of arrival are given in spherical coordinates, where θ is the Zenital Distance and ϕ is the Azimuth in the transformed reference system.

θ tendency is almost equivalent for both receivers because of the predominant component is again the altitude with respect to the ground that is the same for both.

On the other hand, when we take into account ϕ, the trend changes. Differently from what we said for θ the results change between the receivers, in fact the peculiar length of one side of the building with respect to the other one becomes an important element during the transmitter deployments and consequently it adds variance to the simulation outputs.

It is clear that city environment and building construction characteristics have a strong impact on propagation properties and on the distributions of the direction of arrival (but also of received power), which makes the development of ad hoc models and the correct adaptation of existing models a difficult task.

In this sense future works could develop models that, including the urban environment characteristics in an indoor-to-outdoor transmission, depend on

the relative position of the drone w.r.t to the floors in order to simplify and speed up radio coverage estimation.
Connected to what I had the chance to verify in my work, some considerations need to be made regarding the floor in which the transmitter is located. Indeed, would be useful to observe how the distribution changes both by varying the drones altitudes and considering even more floors beyond those I examined with the UAV positioned over the rooftop, but also adding more buildings to get a more complicated environment.
Also, the introduction of the interference caused by the transmitters themselves can constitute an additional step in the development of my work since in my case the transmitters have been considered independently from each other. A further step that could be taken into account is the introduction of the interference caused by the transmitters themselves, as in my case they were considered independent from each other.
Another future improvement can be linked to the user localization aspect. In fact it is necessary to develope techniques that allow to extract positional information from the received signals especially in tough wireless propagation environments, which could allows to quickly identify trapped people with a sufficient level of accuracy and precision.

Bibliography

[1] K. K. F. C. Matteo Coronese, Francesco Lamperti and A. Roventini, "Evidence for sharp increase in the economic damages of extreme natural disasters." *PNAS*, vol. 116, no. 43, pp. 21 450–21 455, 2019.

[2] A. Ranjan, B. Panigrahi, H. K. Rath, P. Misra, A. Simmha, and H. Sahu, "A study on path loss model for uav based urban disaster and emergency communication systems," 02 2018.

[3] S.-K. Noh and D. Choi, "Propagation Model in Indoor and Outdoor for the LTE Communications." *International Journal of Antennas and Propagation*, 2019.

[4] A. F. e Paolo Mataloni. (2017) Riflessione e rifrazione delle onde elettromagnetiche.

[5] M. Santarsiero. (2017/2018) Trasmissione e riflessione di onde piane da strato dielettrico. [Online]. Available: http://webusers.fis.uniroma3.it/ ottica/sant/ottica/pdffiles/Strato.pdf

[6] Y. S. Meng and Y. H. Lee, "Measurements and characterizations of air-to-ground channel over sea surface at c-band with low airborne altitudes," *IEEE Transactions on Vehicular Technology*, vol. 60, pp. 1943–1948, 2011.

[7] J. Meinilä, P. Kyösti, T. Jämsä, and L. Hentila, *WINNER II Channel Models*, 09 2009, pp. 39–92.

[8] A. Al-Hourani, K. Sithamparanathan, and A. Jamalipour, "Modeling air-to-ground path loss for low altitude platforms in urban environments," *2014 IEEE Global Communications Conference*, pp. 2898–2904, 2014.

[9] P. Rademacher. Ray tracing: Graphics for the masses. [Online]. Available: https://www.cs.unc.edu/ rademach/xroads-RT/RTarticle.html

[10] L. Ferreira, B. Kuipers, C. Rodrigues, and L. Correia, "Characterisation of signal penetration into buildings for gsm and umts," 10 2006, pp. 63 – 67.

[11] Q. Feng, E. Tameh, A. Nix, and J. Mcgeehan, "Wlcp2-06: Modelling the likelihood of line-of-sight for air-to-ground radio propagation in urban environments," 01 2007, pp. 1 – 5.

[12] Q. Feng, J. Mcgeehan, E. Tameh, and A. Nix, "Path loss models for air-to-ground radio channels in urban environments," 06 2006, pp. 2901 – 2905.

[13] *Wireless InSite Reference Manual.*

[14] N. S. Software. (2020) Introduction to curve fitting. [Online]. Available: https://ncss-wpengine.netdna-ssl.com/wp-content/themes/ncss/pdf

[15] I. Poole. (2020) Electronics notes, radio receiver sensitivity. [Online]. Available: https://www.electronics-notes.com/articles/radio/radio-receiver-sensitivity/basics.php

[16] H. Enterprise. (2020) Receiver sensitivity.

[17] K. Ukhurebor and C. Abiodun, "Assessment of building penetration loss of cellular network signals at 900 mhz frequency bands in otuoke, bayelsa state, nigeria," vol. 119, 06 2018.

[18] G. Verma, F. T. Dagefu, B. M. Sadler, and J. Twigg, "Direction of arrival estimation with the received signal strength gradient," *IEEE Transactions on Vehicular Technology*, vol. 67, no. 11, pp. 10 856–10 870, 2018.

[19] A. Conti, S. Mazuelas, S. Bartoletti, W. C. Lindsey, and M. Z. Win, "Soft information for localization-of-things," *Proceedings of the IEEE*, vol. 107, no. 11, pp. 2240–2264, 2019.